Open access • Journal Article • DOI:10.1016/J.COLSURFB.2016.03.076

Colloidal mesoporous silica nanoparticles enhance the biological activity of resveratrol — Source link

Natalie Summerlin, Zhi Qu, Naisarg Pujara, Yong Sheng ...+3 more authors

Institutions: University of Queensland

Published on: 01 Aug 2016 - Colloids and Surfaces B: Biointerfaces (Elsevier)

Topics: Mesoporous silica and Resveratrol

Accepted Manuscript

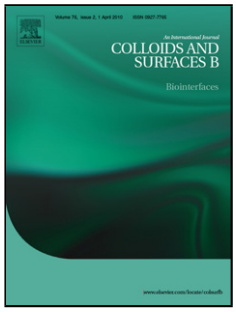

Title: Colloidal Mesoporous Silica Nanoparticles Enhance the Biological Activity of Resveratrol

Author: Natalie Summerlin Zhi Qu Naisarg Pujara Yong Sheng Siddharth Jambhrunkar Michael McGuckin Amirali Popat

PII: S0927-7765(16)30231-4
DOI: http://dx.doi.org/doi:10.1016/j.colsurfb.2016.03.076
Reference: COLSUB 7783

To appear in: *Colloids and Surfaces B: Biointerfaces*

Received date: 8-1-2016
Revised date: 16-2-2016
Accepted date: 25-3-2016

Please cite this article as: Natalie Summerlin, Zhi Qu, Naisarg Pujara, Yong Sheng, Siddharth Jambhrunkar, Michael McGuckin, Amirali Popat, Colloidal Mesoporous Silica Nanoparticles Enhance the Biological Activity of Resveratrol, Colloids and Surfaces B: Biointerfaces http://dx.doi.org/10.1016/j.colsurfb.2016.03.076

Colloidal Mesoporous Silica Nanoparticles Enhance the Biological Activity of Resveratrol

Natalie Summerlin,[a] Zhi Qu,[a] Naisarg Pujara,[a] Yong Sheng,[b] Siddharth Jambhrunkar,*[b] Michael McGuckin*[b] and Amirali Popat*[ab.]

[a]The School of Pharmacy, The University of Queensland, Brisbane, QLD 4072, Australia
[b]Mucosal Diseases Group, Mater Research Institute – The University of Queensland, Translational Research Institute, 37 Kent St, Woolloongabba, QLD 4102

Corresponding Author Email: a.popat@uq.edu.au
Phone: +61(7) 33461870
Number of words: 5360 including reference
Number of tables and figures: 6 (attached in figures section)
Supplementary Figures: 1figure and 1 table

Abstract:

The naturally occurring polyphenol resveratrol (RES) has attracted increasing attention in recent years due to its antioxidant, anti-inflammatory, and anticancer activity. However, resveratrol's promising potential as a nutraceutical is hindered by its poor aqueous solubility, which limits its biological activity. Here we show that encapsulating resveratrol in colloidal mesoporous silica nanoparticles (MCM-48-RES) enhances its saturated solubility by ~95% and increases its *in vitro* release kinetics compared to pure resveratrol. MCM-48-RES showed high loading capacity (20% w/w) and excellent encapsulation efficiency (100%). When tested against HT-29 and LS147T colon cancer cell lines, MCM-48-RES-mediated *in vitro* cell death was higher than that of pure resveratrol, mediated via the PARP and cIAP1 pathways. Finally, MCM-48-RES treatment also inhibited lipopolysaccharide-induced NF-κB activation in RAW264.7 cells, demonstrating improved anti-inflammatory activity. More broadly, our observations demonstrate the potential of colloidal mesoporous silica nanoparticles as next generation delivery carriers for hydrophobic nutraceuticals.

Key Words: resveratrol, mesoporous silica, anticancer, nanoparticles, colorectal cancer, anti-inflammatory

Introduction

Whilst research and development into cancer therapies has intensified in recent decades and significant advancements in cancer treatments have been made, cancer remains the leading cause of disease burden in Australia[1, 2]. Key challenges in treatment include poor solubility of drugs and lack of site specific delivery to cancer cells, development of drug resistance in cancer cells, and adverse effects due to poor drug targeting[3, 4]. Consequently, the search continues for novel drug delivery technologies with better targeting and reduced toxicity. Colorectal cancer is the second most common cause of cancer in males and third most common in females, accounting for 8% of all cancer deaths[5]. Diet is associated with risk of development of colon cancer, hence there is great interest in dietary factors that may exert chemopreventive and chemotherapeutic actions[6]. Dietary components contain many bioactive ingredients that are able to regulate multiple molecular pathways involved in cancer development and progression.

Resveratrol (3,5,4'-trihydroxystilbene) (RES) is a naturally occurring polyphenol and phytoalexin, which is produced by plants in response to environmental stress such as fungal infections, injury and UV irradiation[7-10]. RES can also be found in many foods commonly consumed in the human diet such as red wine, grapes and peanuts[11, 12]. In recent years RES has attained significant attention due to its various therapeutic effects including antioxidant, cardioprotective, anti-inflammatory and anticancer activity, however, RES suffers from many pharmacokinetic limitations[13-15].

RES is a Biopharmaceutics Classification System (BCS) class II drug with poor aqueous solubility (0.03g/L) and a partition coefficient (log $P_{o/w}$) of 3.1[16-18]. RES exists in two geometric isomers, *cis*- and *trans*-, with the latter being more abundant and biologically active[19-21]. However, when exposed to light *trans*-resveratrol undergoes photoisomerization to *cis*-resveratrol[22, 23]. Whilst the oral absorption of RES in humans is high (≈75%), the drugs bioavailability is less than 1% as a result of erratic absorption in the gut and extensive first pass metabolism in the intestine and liver[24, 25]. Walle *et. al.*[25] observed RES had a half life of 9.2 hours in humans with two peak plasma concentrations, after one and six hours. Together these poor

pharmacokinetic properties severely hinder resveratrol's potential as a therapeutic agent. [26]

Nanocarriers are advantageous in cancer therapy due to the enhanced permeation and retention effect (EPR) whereby nano-size particles accumulate preferentially in cancer tissue due to wider than usual capillary fenestrations[27, 28]. This phenomenon enables lower drug concentrations to be used, hence reducing the potential for adverse effects. Healthy cells are less affected due to drug targeting, which ensures localized drug action in tumors. Additionally, nanocarriers increase bioavailability of poorly soluble drugs by increasing solubility and peak plasma concentration of the drug in the blood following uptake via M-cells.[29] Several studies have attempted to improve RES's physicochemical properties by incorporating it into various nanocarriers including liposomes[30, 31], cyclodextrins[32, 33], solid lipid nanoparticles[34], polymeric micelles[35] and polymeric nanoparticles[36]. However, these formulations suffer from drawbacks such as poor stability (e.g. liposomes[37]), low drug loading (e.g. polymers and liposomes 2-10%[36, 37]) and high production costs (e.g. cyclodextrins and polymers[38, 39]). Hence, there is a pressing need for superior cost effective delivery carriers for nutraceuticals such as RES.[26]

Mesoporous silica nanoparticles (MSNs) are biocompatible, have large surface areas and pore volumes and are able to be functionalized making them an ideal shuttle for poorly water-soluble drugs[40-44]. MSNs are regarded as next generation pharmaceutical carriers due to their ability to enhance the efficacy of drugs by improving their aqueous solubility, altering release kinetics, and by targeting via functionalisation. Many recent studies have shown that MSN's improve the aqueous solubility, bioavailability and cell cytotoxicity of hydrophobic drugs such as curcumin, griseofulvin and cyclosporine A [40, 41, 45-48]. However, to the best of our knowledge there is no report on successful encapsulation of RES in MSNs.

In this study, we report the first example of RES encapsulation within MSNs and study its saturated solubility, drug release, anti-inflammatory and anticancer efficacy against colon cancer cells. MCM-48 type MSNs were chosen for this study since they displayed a number of desirable features, including: mono dispersed particle size (150-200 nm), high surface area (~1200

m^2/g), large pore volume (0.9 cm^3/g) highly ordered three dimensional cubic structure of bidirectional mesoporous channels and their ability to encapsulate large amounts of drug[49, 50]. Additionally, our group and others have used MSNs effectively as nanosuspensions and orally delivered tablets, showing their applicability to multiple dosage forms[51]. In this report we describe RES encapsulation in mesoporous silica nanospheres (MCM-48) achieving 20% w/w drug loading, and test their efficacy in a variety of biological assays. We hypothesise that these particles can be used both intravenously as nanosuspensions and/or orally by forming tablets to enhance the overall nutraceutical efficacy and applicability of RES.

Experimental

Materials

Cetyltrimethylammonium bromide (CTAB), tetraethylorthosilicate (TEOS), phosphate buffered saline (PBS), Pluronic F127 (PF127), hydrochloric acid 32% (HCl), ammonium hydroxide 28% (NH_4OH), ethanol 100% and methanol were purchased from Sigma-Aldrich Australia. Resveratrol was provided as a gift sample by MegaResveratrol, USA. CellTiter 96® AQueous One Solution Cell Proliferation Assay (MTS) was purchased from Promega. DMEM: F12 media was purchased from Sigma and fetal calf serum was purchased from Life Technologies.

Physicochemical Characterisation

Particle size, polydispersity index and zeta potential were measured using a Malvern Zetasizer Nano-ZS. Transmission Electron Microscopy (TEM) images were obtained using a JEOL 1010 microscope operated at 100 kV. Thermogravimetric analysis (TGA) was performed using a Mettler Teledo instrument with a heating rate of 5°C/min in airflow. RES concentration was determined using a UV-VIS spectrophotometer (Varian Cary 50 Bio) at 305nm. X-ray diffractograms were recorded using a Rigaku Miniflex X-ray diffractometer with Fe-filtered Co radiation (λ = 1.79 Å). Nitrogen physisorption measurements were performed at -196 °C using a Micromeritics Tristar II 3020 system.

Synthesis of MCM-48

MCM-48 synthesis was performed with slight modifications to the method reported by Kim *et. al.*[52]. In a typical synthesis, 425 mL of NH_4OH (2.8%) and 170 mL of ethanol were transferred into a 1 L glass bottle to which, 2.0 g of CTAB and 8.0 g of PF127 was added and stirred at 500 rpm until dissolved. The speed of stirring was increased to 850 rpm and 7.203 g of TEOS was quickly added to the solution whilst stirring at this speed for 1 min. The solution was then left in static condition for a further 24 h at room temperature. The resulting white product was isolated using high-speed centrifugation (15,000 rpm for 15 min), redispersed once in Milli-Q water and then twice in ethanol and dried at 60 °C overnight. The MCM-48 was then calcined (air, 550 °C, 1 °C/min) for 5.5 h.

Resveratrol loading

Resveratrol loading was performed using a rotary evaporation technique with slight modifications to the procedure reported by Jambhrunkar *et al.*[41]. 40 mg of RES was placed in rotary evaporation flask with 10 mL of ethanol and sonicated for 2 min. 160 mg of MCM-48 was then added and sonicated for a further 5 min. The solvent was slowly evaporated using rotary evaporator at 50 °C to obtain RES loaded MCM-48 (MCM-48-RES) with 20% w/w theoretical drug loading. The evaporation process was continued until all ethanol was removed and a dry powder was observed in the flask. This sample was collected, stored covered in aluminum foil to protect it from photo degradation and used for further studies.

Solubility and *in vitro* release

We performed saturated solubility studies by adding an excessive quantity (0.5 mg equivalent) of RES, MCM-48 and RES physical mixture (PM) and MCM-48-RES to 0.5 mL of Milli-Q water. This mixture was kept shaking for 48 h at 37 °C whilst protected from light. The suspension was then centrifuged, diluted

with deionized water and the supernatant was analysed for RES content using UV-VIS spectroscopy ($r^2 = 0.999$) at 305 nm.

The *in vitro* release of RES from MCM-48-RES was conducted by suspending MCM-48-RES equivalent to 1 mg of RES in 1 mL of PBS (pH 7.4) This suspension was placed in a snakeskin dialysis bag with a 10 kDa molecular weight cut-off and immersed into 9 mL of PBS at 37 °C whilst continually stirring. At predetermined time intervals 1 mL of the sample was withdrawn and immediately replaced with an equal volume of PBS to maintain sink conditions. The removed samples were analyzed for RES content using UV-VIS spectroscopy ($r^2 = 0.997$) at 305 nm.

***In vitro* cytotoxicity assay**

HT-29 and LS174T cell lines were propagated in monolayers to sub-confluency at 37 °C in 75 cm^2 flasks containing 10 ml of DMEM: F12 media, supplemented with heat inactivated 10% foetal calf serum (FCS), 1% penicillin, 1% glutamine and 1% streptomycin in a fully-humidified incubator containing 5% CO_2 and 95% air. The sensitivity of these cells to the RES in MCM-48 was determined using a MTS colorimetric assay. Cells (0.5×10^4 per well) were seeded in a flat-bottomed 96-well plate and incubated at 37 °C in 5% CO_2. Cells were exposed to RES in DMSO and MCM-48 nanoparticles alone or loaded with RES at concentrations of 100, 200 and 400 μM in a dose dependent manner for 48 h. Cells were then treated with MTS reagent (20 μL/well) for 3 h at 37 °C. The optical density (OD) was recorded at 490 nm in a microplate reader and percentage of residual cell viability was determined. Control cells, DMSO carrier and MCM-48 not loaded with drugs were used as negative controls and Triton-X100 was used as a positive control for death of all cells.

Immunoblot analysis

HT-29 and LS174T cells were seeded in 6-well culture plate at 80% confluence. After overnight attachment, HT29 and LS174T cells were treated with 200 μM RES, RES in DMSO or MCM48-RES. Then cells were collected, washed twice with cold PBS, pH 7.4 and then lysed on ice for 15 min with RIPA cell lysate buffer (RIPA buffer: 50 mM Tris-HCI, pH 7.5, 150 mM NaCl,

1.0 % Nonidet P-40, 0.1% sodium deoxycholate, and 1.0% protease inhibitor cocktail) while stirring every 5 min. The resulting lysates were centrifuged at 16,000 g for 20 min at 4°C to remove cell debris. Aliquots of the cell lysates from each treatment condition were resuspended in SDS-PAGE Laemmli buffer (0.05M Tris-HCI, pH 6.8, 2.55M 2-mercaptoethanol, 1.0% SDS, 5% glycerol, and 0.15M bromophenol blue), boiled for 5 min at 100 °C, and resolved on 4-12% acrylamide gels. Resolved proteins were transferred to polyvinylidene difluoride (PVDF) membranes, probed with anti-β-actin (Novus Biologicals, Littleton, CO 80160, USA), anti-PARP (cat no 9542, Cell Signaling Technology), anti-cleaved caspase-3 (Asp175, cat no 9915 Cell Signaling Technology), anti-cIAP1 (cat no 7065, Cell Signaling Technology) antibodies. Immunoreactive proteins were detected by dual-label infra-red analysis using an Odyssey scanner.

***In-vitro* anti-inflammatory assay**

RAW 264.7 macrophage cells transfected with the NF-kB-responsive ELAM1 promoter driving GFP[53] were seeded at 15,000 cells/well in 96 well plate in a fully-humidified incubator containing 5% CO_2 and 95% air. After overnight incubation, to study the effect of RES on inhibition of NF-kB, cells were pre-treated with 200 μM RES suspension, RES in DMSO, or MCM-48-RES for 6 h and then 5 ng/mL LPS was added to the cells to activate NF-kB. After overnight incubation cells were washed with phosphate buffer saline and the amount of GFP expressed was measured using fluorescence microscopy. To avoid any fluorescence interference due to nanoparticles, MCM-48 was included in this assay as negative control.

Results and Discussion

Physicochemical characterisation

The physical properties of MCM-48 and MCM-48-RES did not differ significantly. The TEM images displayed in Fig 1a and 1b are typical of MCM-48 and allow the visualisation of its cubic pores in an ordered array. Dynamic light scattering (DLS) measurements shown in the Fig 1a insert reveal a mean hydrodynamic diameter of 191nm and 283nm for MCM-48 and MCM-48-RES,

respectively. The polydispersity index (PDI) of 0.06 reveals MCM-48 particles are monodisperse. After drug loading the PDI of MCM-48-RES increases to 0.25, possibly due to drug release while measuring particle size and PDI in aqueous suspension. Although, the PDI of MCM-48-RES has increased to 0.25, the unimodal particle size distribution indicates homogeneity. Additionally, the zeta potentials of -28.2 mV and -22.2 mV for MCM-48 and MCM-48-RES, respectively, suggest that nanoparticles are colloidally stable (Electronic Supplementary Information-ESI Table S1).

The X-ray diffractometry (XRD) pattern of MCM-48 in Fig 1c shows two well-resolved diffraction peaks at 211 and 220, which confirms the symmetry to be *Ia3d*. The nitrogen adsorption/desorption isotherms of MCM-48 in Fig 1d show sharp capillary condensation at 0.4 (P/Po) and a type IV isotherm as previously reported for MCM-48. After drug loading the surface area was decreased from ~1100 m^2/g to 729 m^2/g indicating encapsulation of RES. Thermogravimetric analysis (TGA) analysis was used to determine the drug loading in the nanoparticles (Fig 2a). The results show ~21% of RES was encapsulated indicating the high efficiency of the rotary evaporation technique for drug loading, consistent with previous studies[41, 54, 55]. The Differential scanning calorimetry (DSC) curve of RES, MCM-48 and MCM-48-RES are presented in Fig 2b. This analysis was performed to examine the crystallinity of RES after encapsulation in pores of MCM-48. Pure RES displayed a sharp endothermic peak at 268 °C representing its crystalline structure with a sharp melting point. No such peak was observed in MCM-48-RES indicating RES was in a non-crystalline state, thus suggesting successful loading into the nanopores of MCM-48. Additionally, no solvent endothermic peak was observed in MCM-48-RES confirming successful removal of organic solvent during the drug loading process. The amorphous nature of RES within nanopores of MCM-48 was further studied using wide angle XRD. As shown in Fig. 3 RES shows sharp diffraction peaks between 15-30^o indicative of its crystalline nature in its free powdered form. These peaks were also visible at a lower intensity in a physical mixture of MCM-48 and RES, suggesting incomplete encapsulation. However, such diffraction peaks were absent in both MCM-48 and MCM-48-RES demonstrating the amorphous nature of RES

within nanoparticles. These results are in good agreement with the DSC results, confirming the successful loading of drug into the silica particles.

Solubility and *in vitro* drug release studies

Poor solubility profile is one of the key formulation challenges facing drug development, with more than 60% of new chemical entities showing poor aqueous solubility. The solubility of RES was determined by preparing saturated solutions of RES and MCM-48-RES in water to reach the equilibrium concentration. Fig. 4a shows RES solubility was significantly enhanced approximately 2 fold ($P<0.0001$) in MCM-48-RES (106.1 μg/mL) compared to RES (54.2 μg/mL). Moreover, solubility was also significantly higher in MCM-48-RES than its physical mixture MCM-48-RES-PM (74.2 μg/mL, $P<0.0001$). The enhanced solubility of RES is attributed to the confinement of RES in mesochannels (~2.1nm) in small size and amorphous form confirmed by DSC and XRD studies. As described by the Ostwald-Freundlich equation, as particle size decreases surface area increases and hence the saturated solubility also increases[56].

Apart from solubility, the drug release kinetic is also an important parameter in predicting *in-vivo* activity. The improved solubility of RES from MCM-48-RES can also be observed through the *in vitro* drug release results using PBS as the dissolution medium (Fig. 4b). After 30 min, MCM-48-RES exhibited 36.9% drug dissolution whereas RES released only 15.6% over the same period. The rate of drug release for RES alone was 31.3% after 24 h, which was much slower than MCM-48-RES, which gave a release profile of 64.7% after 24 hours. The increased dissolution rate of RES from MCM-48-RES could be attributed to the amorphous state of RES within cubic pores of MCM-48 and the higher surface area provided by colloidal nanoparticles resulting faster diffusion and release.

Cell studies

To evaluate the relative anticancer efficacy of free and nanoparticle-encapsulated RES, cell cytotoxicity studies using the MTS metabolic activity assay were conducted on HT-29 and LS174T colon cancer cell lines (Fig. 5). These cell lines were chosen as previous studies have examined free RES's

ability to induce cell death in colon cancer cells, such as HT-29 cells[6, 58]. All studies were conducted over 48 hours. MCM-48 nanoparticles alone as control showed almost no cytotoxicity in both cell lines, indicating their lack of toxicity consistent previous studies[59]. Both cell lines were treated with three concentrations (100, 200 and 400 μM) of RES in dimethyl sulfoxide (DMSO) and MCM-48-RES. DMSO was chosen as it is a solvent which readily dissolves the drug however, cannot be used as a drug delivery agent due to its adverse effects in humans including organ damage. Both RES in DMSO and MCM-48-RES showed dose dependent decreases in cellular metabolism in both cell lines, consistent with alterations in mitochondrial metabolism, decreased cell proliferation or increased apoptosis. For example, the cell viability in LS174T cells after being treated with MCM-48-RES 100 μM was 84%, when the concentration was increased to 200 μM and 400 μM the cell proliferation reduced to 57% and 28%, respectively. A similar trend was observed in HT-29 cells, but the difference between pure RES and MCM-48-RES was not as high, especially at lower concentrations. LS174T cells appear to be more sensitive to RES compared to HT-29 cells with 28% cell viability was after being treated with MCM-48-RES 400 μM, compared to ~36% in HT-29 cells. From the results it can be concluded that MCM-48-RES appears to be as effective as RES in DMSO at inducing cell death in both cell lines.

The comparable cytotoxicity of MCM-48-RES could be attributed to the enhanced solubility and superior release kinetics of RES from the MCM-48-RES as demonstrated in the Fig. 5. However, MTS assay alone cannot corroborate the apoptosis induced by RES and also nanoparticles may also have some interference with absorbance too. To examine the induction of apoptosis we used Western blotting to evaluate cleavage of PARP and clAP1 in cells treated with RES suspension, RES-DMSO and MCM-48-RES (Fig 6). Treatments with MCM-48-RES led to a substantial increase in PARP in HT29 and LS174T cell lines (Fig 6) compared to other treatments. Consistent with this observation, we found that the treatment with MCM-48-RES substantially decreased intracellular apoptosis protein I (cIAP1) expression in both cell lines. Interestingly, RES suspension showed some decreased in cIAP1, however RES-DMSO groups showed little impact on apoptosis. It is noteworthy that in case

of HT-29 cells, blank MCM-48 nanoparticles slightly increased PARP, which warrants further investigation.

To assess the potential of RES as an anti-inflammatory agent we used a NF-kB activation assay using RAW 264.7 reporter cells. RES decreases inflammation by down regulating several pathways including NF-kB, a phenomenon that is very well documented.[60] However, due to poor solubility, very high doses need to be administered to achieve the desired anti-inflammatory benefits. Hence, we decided to test the effect of our MCM-48-RES, RES suspension and RES-DMSO on down regulation of NF-kB using LPS-activated RAW 264.7 cells (Please refer to ESI-Fig S1). As shown in Fig S1b RAW cells activated by LPS show extremely high fluorescence due to expression of GFP. Cells pre-treated with 100 μM RES (Fig S1c-e), on the other hand, showed overall decrease in fluorescence signal. As expected at 100μM RES concentration, MCM-48-RES showed significantly less green fluorescence than with RES suspension or RES-DMSO (Fig S1g), further affirming superiority of our formulation. It is worthy to note that MCM-48 alone (Fig S1f) showed minimal autofluorescence confirming the effect is due to high release and improved solubility of RES from our nanoformulation.

Conclusions

In summary, we have prepared RES loaded MCM-48 nanoparticles using a simple yet efficient technique to explore the effect on solubility and *in vitro* drug release, as well as anti-inflammatory and anticancer activity using *in-vitro* assays. It was found that when RES was encapsulated in MCM-48 the solubility increased almost two-fold. Additionally, MCM-48-RES showed enhanced dose-dependent cytotoxicity comparable with RES in DMSO in both cell lines. The higher rate of apoptosis caused by MCM-48-RES was further confirmed by immune blotting for proteins in the apoptosis pathway. Interestingly, MCM-48-RES showed significantly greater suppression of LPS-stimulated NF-kB in macrophages compared to RES in aqueous suspension. Based on these results it can be concluded that MSN serves as a promising nanocarrier for RES. The findings from this study provide novel insights into MSNs as a drug delivery carrier for hydrophobic drugs, while also adding to

the established body of evidence regarding the usefulness of RES as an anticancer drug. Future studies will involve examining various types of MSNs and testing the effects of surface functionalization on solubility, *in vitro* release, cytotoxicity and endocytosis.

Acknowledgements:

We thank The National Health and Medical Research Council's Early Career Fellowship to A. Popat and Principal Research Fellowship to M. McGuckin, and The University of Queensland for financial support. The Translational Research Institute is supported by a grant from the Australian Government. We acknowledge the Australian Microscopy and Microanalysis Research Facility at the Centre for Microscopy and Microanalysis, The University of Queensland. We also would like to thank Tan Nguyen, Anand Meka, and Jun Zhang for minor technical assistance.

References:

[1] Wyatt SW, Sands HR, Maynard WR, Humbaugh KE. All cancers age-adjusted mortality rate surpasses diseases of the heart. Journal of Cancer 2012;3:113-6.
[2] (AIHW) AIoHaW. Australian Cancer Incidence and Mortality (ACIM) books: All cancers combined. Canberra: AIHW; 2014.
[3] Yang XI, Cheng Y, Luo N, Gong C. Nanomedicine to Overcome Cancer Multidrug Resistance. Current drug metabolism 2014.
[4] Alexis F, Pridgen EM, Langer R, Farokhzad OC. Nanoparticle technologies for cancer therapy. Handbook of experimental pharmacology 2010:55-86.
[5] Society AC. Global cancer facts & figures. 2nd ed. Atlanta: American Cancer Society Inc.; 2011.
[6] Miki H, Uehara N, Kimura A, Sasaki T, Yuri T, Yoshizawa K, et al. Resveratrol induces apoptosis via ROS-triggered autophagy in human colon cancer cells. International journal of oncology 2012;40:1020-8.
[7] Guo W, Li A, Jia Z, Yuan Y, Dai H, Li H. Transferrin modified PEG-PLA-resveratrol conjugates: in vitro and in vivo studies for glioma. European journal of pharmacology 2013;718:41-7.
[8] Ndiaye M, Kumar R, Ahmad N. Resveratrol in cancer management: where are we and where we go from here? Annals of the New York Academy of Sciences 2011;1215:144-9.
[9] Burns J, Yokota T, Ashihara H, Lean ME, Crozier A. Plant foods and herbal sources of resveratrol. Journal of Agricultural and Food Chemistry 2002;50:3337-40.
[10] Neves AR, Lucio M, Lima JLC, Reis S. Resveratrol in medicinal chemistry: a critical review of its pharmacokinetics, drug delivery, and membrane interactions. Current Medicinal Chemistry 2012;19:1663-81.
[11] Karthikeyan S, Rajendra Prasad N, Ganamani A, Balamurugan E. Anticancer activity of resveratrol-loaded gelatin nanoparticles on NCI-H460 non-small cell lung cancer cells. Biomedicine & Preventitive Nutrition 2013;3:64-73.
[12] Caddeo C, Teskac K, Sinico C, Kristl J. Effect of resveratrol incorporated in liposomes on proliferation and UV-B protection of cells. International journal of pharmaceutics 2008;363:183-91.
[13] Yang X, Li X, Ren J. From French Paradox to Cancer Treatment: Anti-cancer Activities and Mechanisms of Resveratrol. Anti-cancer agents in medicinal chemistry 2014.
[14] Aluyen JK, Ton QN, Tran T, Yang AE, Gottlieb HB, Bellanger RA. Resveratrol: Potential as anticancer agent. Journal of Dietary Supplements 2012;9:45-56.
[15] Kraft TE, Parisotto D, Schempp C, Efferth T. Fighting cancer with red wine? Molecular mechanisms of resveratrol. Critical reviews in food science and nutrition 2009;49:782-99.
[16] Mattarei A, Azzolini M, Carraro M, Sassi N, Zoratti M, Paradisi C, et al. Acetal derivatives as prodrugs of resveratrol. Molecular Pharmaceutics 2013;10:2781-92.
[17] Information NCfB. PubChem Substance Database; SID 6374.
[18] Seljak KB, Berginc K, Trontelj J, Zvonar A, Kristl A, Gasperlin M. A Self-Microemulsifying Drug Delivery System to Overcome Intestinal Resveratrol Toxicity and Presystemic Metabolism. Journal of pharmaceutical sciences 2014.

[19] Montsko G, Nikfardjam MSP, Szabo Z, Boddi K, Lorand T, Ohmacht R, et al. Determination of products derived from *trans*-resveratrol UV photoisomerisation by means of HPLC-APCI-MS. Journal of Photochemistry and Photobiology A: Chemistry 2008;196:44-50.
[20] Rius C, Abu-Taha M, Hermenegildo C, Piqueras L, Cerda-Nicolas JM, Issekutz AC, et al. Trans- but not cis-resveratrol impairs angiotensin-II-mediated vascular inflammation through inhibition of NF-kappaB activation and peroxisome proliferator-activated receptor-gamma upregulation. Journal of immunology (Baltimore, Md : 1950) 2010;185:3718-27.
[21] Augustin MA, Sanguansri L, Lockett T. Nano- and micro-encapsulated systems for enhancing the delivery of resveratrol. Annals of the New York Academy of Sciences 2013;1290:107-12.
[22] Bonechi C, Martini S, Ciani L, Lamponi S, Rebmann H, Rossi C, et al. Using Liposomes as Carriers for Polyphenolic Compounds: The Case of Trans-Resveratrol. PLOS ONE 2012;7:1-11.
[23] Vian MA, Tomao V, Gallet S, Coulomb PO, Lacombe JM. Simple and rapid method for cis- and trans-resveratrol and piceid isomers determination in wine by high-performance liquid chromatography using chromolith columns. Journal of chromatography A 2005;1085:224-9.
[24] Walle T. Bioavailability of resveratrol. Annals of the New York Academy of Sciences 2011;1215:9-15.
[25] Walle T, Hsieh F, DeLegge MH, Oatis JE, Jr., Walle UK. High absorption but very low bioavailability of oral resveratrol in humans. Drug metabolism and disposition: the biological fate of chemicals 2004;32:1377-82.
[26] Summerlin N, Soo E, Thakur S, Qu Z, Jambhrunkar S, Popat A. Resveratrol nanoformulations: challenges and opportunities. International journal of pharmaceutics 2015;479:282-90.
[27] Maeda H. The enhanced permeability and retention (EPR) effect in tumor vasculature: the key role of tumor-selective macromolecular drug targeting. Advances in enzyme regulation 2001;41:189-207.
[28] Fang J, Sawa T, Maeda H. Factors and mechanism of "EPR" effect and the enhanced antitumor effects of macromolecular drugs including SMANCS. Advances in experimental medicine and biology 2003;519:29-49.
[29] Swarnakar NK, Jain AK, Singh RP, Godugu C, Das M, Jain S. Oral bioavailability, therapeutic efficacy and reactive oxygen species scavenging properties of coenzyme Q10-loaded polymeric nanoparticles. Biomaterials 2011;32:6860-74.
[30] Coimbra M, Isacchi B, van Bloois L, Torano JS, Ket A, Wu X, et al. Improving solubility and chemical stability of natural compounds for medicinal use by incorporation into liposomes. International journal of pharmaceutics 2011;416:433-42.
[31] Soo E, Thakur S, Qu Z, Jambhrunkar S, Parekh HS, Popat A. Enhancing delivery and cytotoxicity of resveratrol through a dual nanoencapsulation approach. Journal of Colloid and Interface Science 2016;462:368-74.
[32] Venuti V, Cannava C, Cristiano MC, Fresta M, Majolino D, Paolino D, et al. A characterization study of resveratrol/sulfobutyl ether-beta-cyclodextrin inclusion complex and in vitro anticancer activity. Colloids and surfaces B, Biointerfaces 2014;115:22-8.
[33] Popat A, Karmakar S, Jambhrunkar S, Xu C, Yu C. Curcumin-cyclodextrin encapsulated chitosan nanoconjugates with enhanced solubility and cell cytotoxicity. Colloids and surfaces B, Biointerfaces 2014;117:520-7.
[34] Teskac K, Kristl J. The evidence for solid lipid nanoparticles mediated cell uptake of resveratrol. International journal of pharmaceutics 2010;390:61-9.
[35] Lu X, Ji C, Xu H, Li X, Ding H, Ye M, et al. Resveratrol-loaded polymeric micelles protect cells from Abeta-induced oxidative stress. International journal of pharmaceutics 2009;375:89-96.
[36] Sanna V, Siddiqui IA, Sechi M, Mukhtar H. Resveratrol-loaded nanoparticles based on poly(epsilon-caprolactone) and poly(D,L-lactic-co-glycolic acid)-poly(ethylene glycol) blend for prostate cancer treatment. Mol Pharm 2013;10:3871-81.
[37] Lu X-Y, Hu S, Jin Y, Qiu L-Y. Application of liposome encapsulation technique to improve anti-carcinoma effect of resveratrol. Drug Development and Industrial Pharmacy 2012;38:314-22.
[38] Parveen S, Sahoo S. Polymeric nanoparticles for cancer therapy. Journal of Drug Targeting 2008;16:108-23.
[39] Szejtli J. Past, present, and future of cyclodextrin research. Pure and Applied Chemistry 2004;76:1825-45.
[40] Santos HA, Peltonen L, Limnell T, Hirvonen J. Mesoporous materials and nanocrystals for enhancing the dissolution behavior of poorly water-soluble drugs. Current pharmaceutical biotechnology 2014;14:926-38.
[41] Jambhrunkar S, Qu Z, Popat A, Karmakar S, Xu C, Yu C. Modulating in vitro release and solubility of griseofulvin using functionalized mesoporous silica nanoparticles. Journal of colloid and interface science 2014;434:218-25.
[42] Popat A, Jambhrunkar S, Zhang J, Yang J, Zhang H, Meka A, et al. Programmable drug release using bioresponsive mesoporous silica nanoparticles for site-specific oral drug delivery. Chemical communications (Cambridge, England) 2014;50:5547-50.
[43] Perez-Esteve E, Ruiz-Rico M, Martinez-Manez R, Barat JM. Mesoporous Silica-Based Supports for the Controlled and Targeted Release of Bioactive Molecules in the Gastrointestinal Tract. Journal of food science 2015;80:E2504-16.
[44] Niut Y, Popatt A, Yu M, Karmakar S, Gu W, Yu C. Recent advances in the rational design of silica-based nanoparticles for gene therapy. Therapeutic delivery 2012;3:1217-37.
[45] Roggers R, Kanvinde S, Boonsith S, Oupicky D. The Practicality of Mesoporous Silica Nanoparticles as Drug Delivery Devices and Progress Toward This Goal. AAPS PharmSciTech 2014.
[46] Yang KN, Zhang CQ, Wang W, Wang PC, Zhou JP, Liang XJ. pH-responsive mesoporous silica nanoparticles employed in controlled drug delivery systems for cancer treatment. Cancer biology & medicine 2014;11:34-43.

[47] Wang Z, Chen B, Quan G, Li F, Wu Q, Dian L, et al. Increasing the oral bioavailability of poorly water-soluble carbamazepine using immediate-release pellets supported on SBA-15 mesoporous silica. International journal of nanomedicine 2012;7:5807-18.
[48] Lodha A, Lodha M, Patel A, Chaudhuri J, Dalal J, Edwards M, et al. Synthesis of mesoporous silica nanoparticles and drug loading of poorly water soluble drug cyclosporin A. Journal of pharmacy & bioallied sciences 2012;4:S92-4.
[49] Izquierdo-Barba I, Martinez A, Doadrio AL, Perez-Pariente J, Vallet-Regi M. Release evaluation of drugs from ordered three-dimensional silica structures. European journal of pharmaceutical sciences : official journal of the European Federation for Pharmaceutical Sciences 2005;26:365-73.
[50] Popat A, Liu J, Hu Q, Kennedy M, Peters B, Lu GQ, et al. Adsorption and release of biocides with mesoporous silica nanoparticles. Nanoscale 2012;4:970-5.
[51] Abbaraju PL, Meka AK, Jambhrunkar S, Zhang J, Xu C, Popat A, et al. Floating tablets from mesoporous silica nanoparticles. J Mater Chem B 2014;2:8298-302.
[52] Kim T-W, Chung P-W, Lin VSY. Facile Synthesis of Monodisperse Spherical MCM-48 Mesoporous Silica Nanoparticles with Controlled Particle Size. Chemistry of Materials 2010;22:5093-104.
[53] Stacey KJ, Young GR, Clark F, Sester DP, Roberts TL, Naik S, et al. The molecular basis for the lack of immunostimulatory activity of vertebrate DNA. Journal of immunology 2003;170:3614-20.
[54] Jambhrunkar S, Karmakar S, Popat A, Yu M, Yu C. Mesoporous silica nanoparticles enhance the cytotoxicity of curcumin. Royal Society of Chemistry 2014;4:709-12.
[55] Guillet-Nicolas R, Popat A, Bridot JL, Monteith G, Qiao SZ, Kleitz F. pH-Responsive NutraceuticalMesoporous Silica Nanoconjugates with Enhanced Colloidal Stability. Angewandte Chemie-International Edition 2013;52:2318-22.
[56] Kaptay G. On the size and shape dependence of the solubility of nano-particles in solutions. International journal of pharmaceutics 2012;430:253-7.
[57] Wang Y, Sun L, Jiang T, Zhang J, Zhang C, Sun C, et al. The investigation of MCM-48-type and MCM-41-type mesoporous silica as oral solid dispersion carriers for water insoluble cilostazol. Drug Dev Ind Pharm 2014;40:819-28.
[58] Fouad MA, Agha AM, Merzabani MM, Shouman SA. Resveratrol inhibits proliferation, angiogenesis and induces apoptosis in colon cancer cells: calorie restriction is the force to the cytotoxicity. Human & experimental toxicology 2013;32:1067-80.
[59] Lu J, Liong M, Li Z, Zink JI, Tamanoi F. Biocompatibility, biodistribution, and drug-delivery efficiency of mesoporous silica nanoparticles for cancer therapy in animals. Small (Weinheim an der Bergstrasse, Germany) 2010;6:1794-805.
[60] Chavez E, Reyes-Gordillo K, Segovia J, Shibayama M, Tsutsumi V, Vergara P, et al. Resveratrol prevents fibrosis, NF-kappaB activation and TGF-beta increases induced by chronic CCl4 treatment in rats. Journal of applied toxicology : JAT 2008;28:35-43.

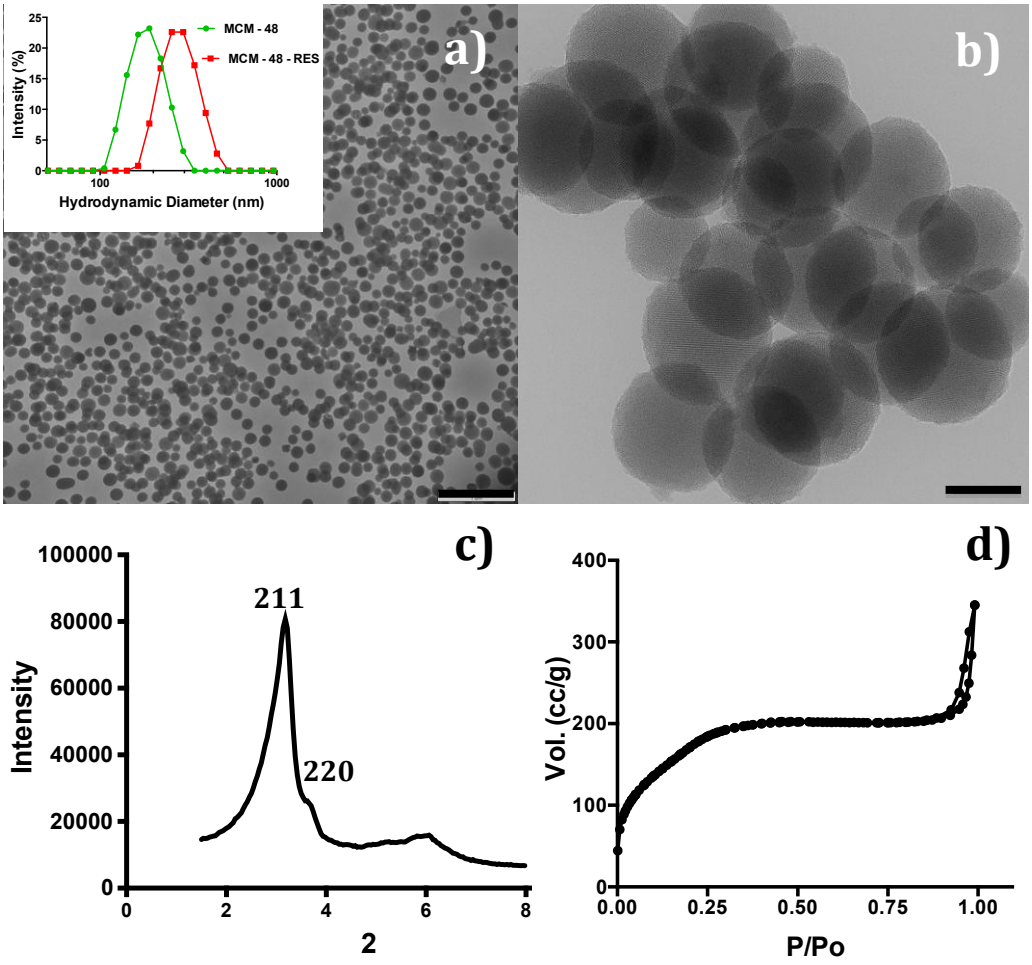

Fig. 1. Transmission electron microscopy images of MCM-48 (a) & (b). Insert figure depicts dynamic light scattering (DLS) measurements of MCM-48 and MCM-48-RES. Small angle X-ray diffraction (XRD) of MCM-48 (c). N_2 adsorption-desorption isotherm of MCM-48 (d). Scale bars: a) 1 μm, b) 150 nm.

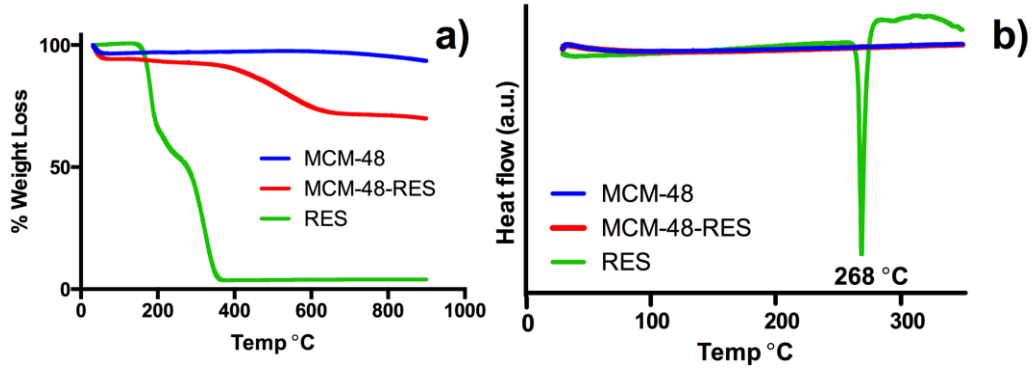

Fig. 2. Thermogravimetric analysis (TGA) (a) and Differential Scanning Colorimetry (DSC) (b) profile of pure RES, MCM-48 and RES loaded MCM-48.

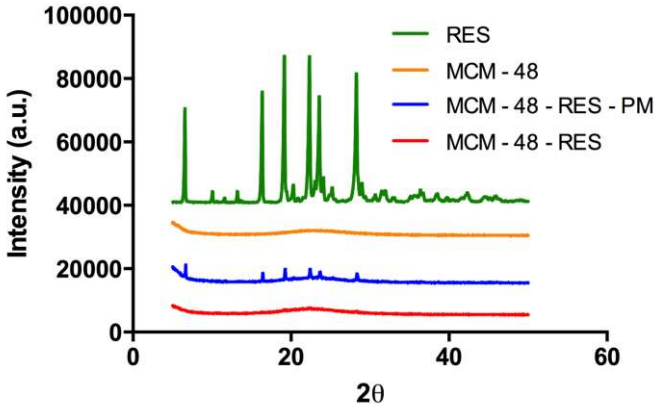

Fig. 3 Wide angle X-ray diffraction (XRD) pattern of RES, MCM-48, MCM-48-RES-PM and MCM-48-RES-physical mixture (PM)

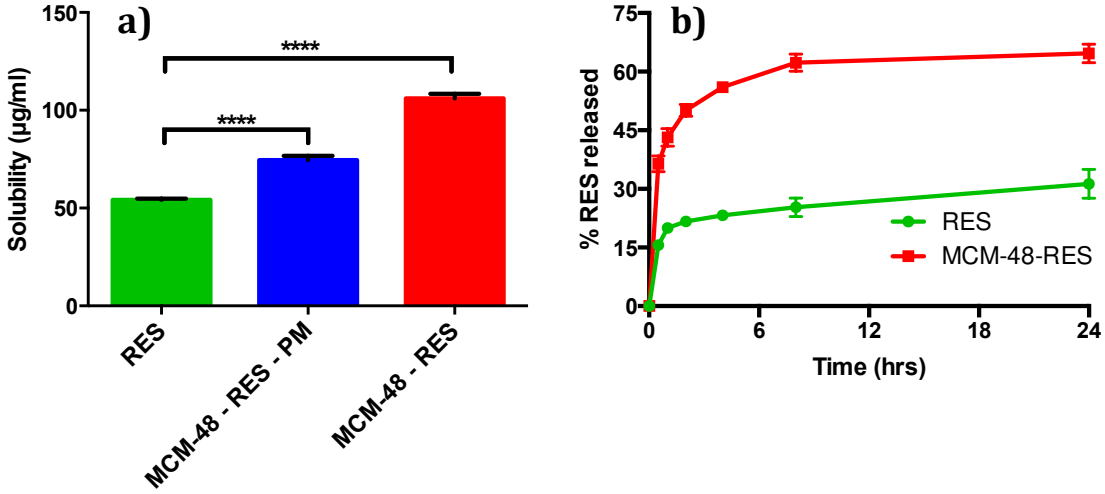

Fig. 4. (a) Saturated aqueous solubility of pure RES, MCM-48-RES-PM and MCM-48-RES (n=3 ±SD, P value was determined by one-way ANOVA, **** P<0.0001), (b) *In vitro* release of pure resveratrol and resveratrol loaded in MCM-48 in phosphate buffer saline (PBS) (n=3 ±SD)

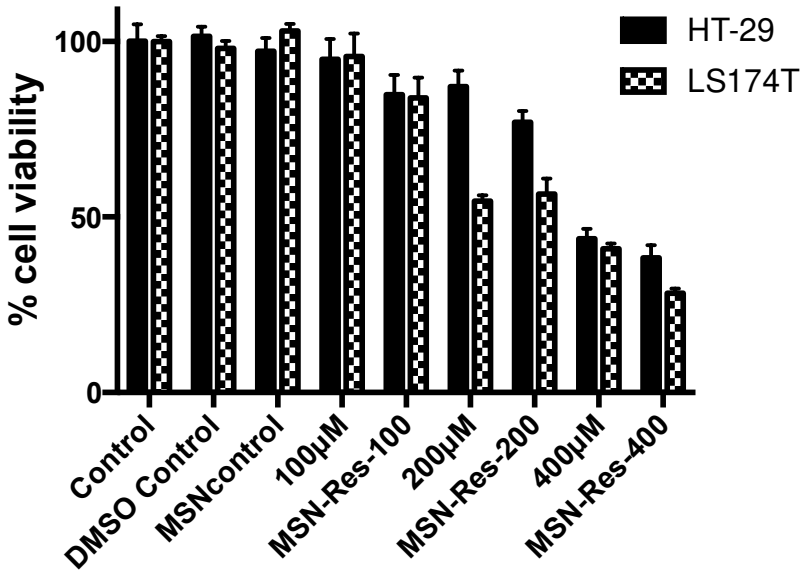

Fig. 5. *In vitro* cytotoxicity of RES in DMSO and MCM-48-RES on HT-29 and LS174T cell lines after 48 hours using MTS assay (n=6 ±SD).

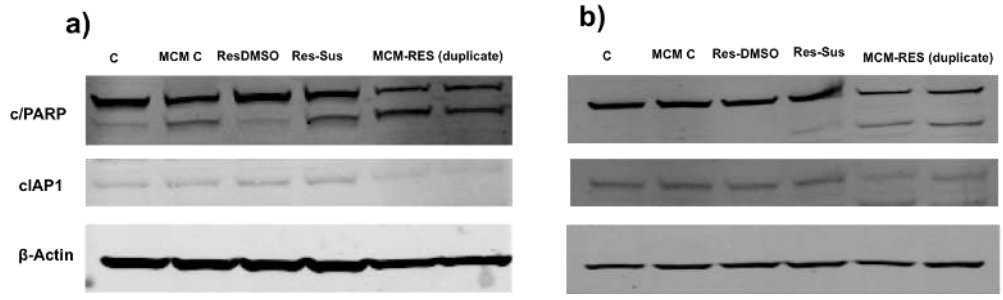

Fig 6. Protein expression studies using total cell lysates with C/PARP, ClAP1, and with β-actin as a loading control by western blot analysis of control (C) MCM-48 particle control (MCM-C), Resveratrol in DMSO and suspension (RES-DMSO, RES-Sus) and Resveratrol encapsulated into MCM-48 (MCM-RES) in a) HT-29 and b) LS147T cells.

Nanoencapsulation of Resveratrol

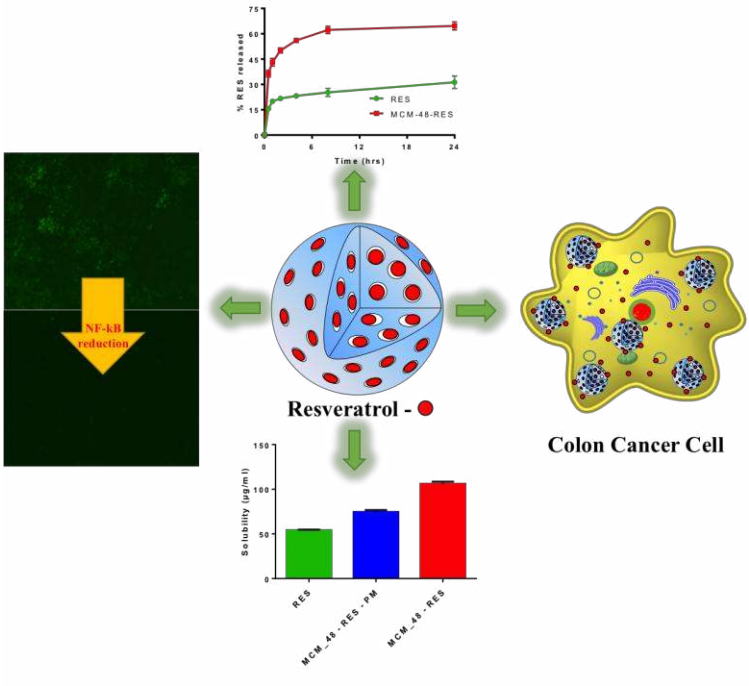

Highlights:

- Resveratrol is encapsulated in mesoporous silica nanoparticles.
- Encapsulation significantly enhanced solubility and drug release.
- Encapsulated Resveratrol showed significantly improved NF-κB reduction.
- Encapsulated Resveratrol caused higher apoptosis compared to pure drug.